Modeling Control and Simulation of a Parallel Hybrid Agricultural Tractor

Davide Tebaldi[1] and Roberto Zanasi[2]

***Abstract*— The modeling, the control and the simulation of a parallel hybrid architecture for an agricultural tractor propulsion system are performed in this paper. The systems involved in the considered architecture are: an Internal Combustion Engine (ICE), two Permanent Magnet Synchronous Motors (PMSMs), a supercapacitor playing the role of the energy storage device, a clutch allowing to enable/disable the electrical power path, and finally the transmission system from the gearbox to the wheels of the vehicle. A control strategy aiming at minimizing the ICE specific fuel consumption is then proposed and tested by presenting some simulation results.**

I. Introduction

The trend in modern vehicles on the road is more and more towards the hybridization of the propulsion system. The potential reduction in terms of exhaust emissions can bring several advantages for all industries working in the automotive and agricultural fields, both in terms of economic return and in terms of improving the environmental sustainability.

In order to develop an effective control strategy for the system, it is necessary to rely upon an effective hybrid vehicle model. This paper deals with the modeling and with the proposal of a control strategy for a parallel hybrid architecture, with the aim of reducing the specific fuel consumption of the endothermic source of energy.

Some of the advantages coming from the employment of a parallel hybrid architecture are reported in [1]. Among such advantages, it is worth mentioning the presence of two parallel power paths from the ICE to the tractor transmission system. The first one is a *direct* mechanical power path, which lets a given fraction of the mechanical power generated by the ICE flow through a gearbox and be delivered to the load. The second one is an *indirect* electrical power path. In this case, a determined fraction of the ICE power undergoes a mechanical-to-electrical energy conversion by means of an electric machine, gets stored in an energy storage device, and eventually undergoes a final electrical-to-mechanical energy conversion performed by another electric machine. The first electric machine plays the role of a generator to recharge the energy storage device. The second electric machine acts as a motor, in order to help the ICE to satisfy the load required power level.

From this qualitative description of parallel hybrid architectures, an important concept turns out: the indirect, electrical path represents a high-frequency power path. The efficiency of the latter is generally lower, due to the two energy conversions taking place along it. Nevertheless, it is the presence of this additional power path that brings an important benefit of parallel hybrid architectures: the decoupling of the ICE torque from the disturbances coming from the load. In a classical fully-mechanical transmission system, neither the ICE speed nor the ICE torque are degrees of freedom. This is due to two facts: the direct proportionality between the ICE speed and the vehicle speed through to the engaged gear, and the ICE torque task of compensating the external torque disturbances. In a parallel architecture, the ICE speed is still related to the vehicle speed, whereas some of the external torque disturbances that come from the load can be compensated by an electric machine acting as a motor, through the indirect electrical power path. As a consequence, the most suitable ICE torque can be exploited as a degree of freedom, while satisfying the constraints.

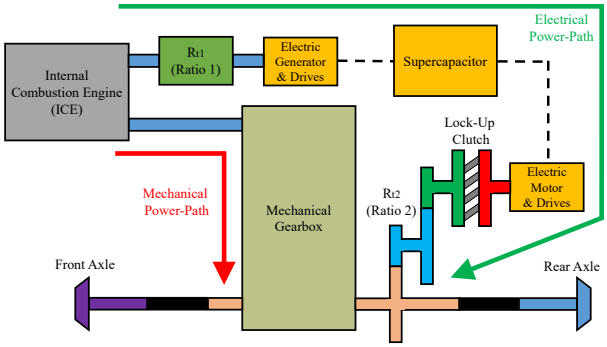

Fig. 1. Considered parallel hybrid propulsion system: structure overview.

A schematic form of the hybrid architecture under consideration is given in Fig. 1. From the figure, the reader can appreciate the presence of the two power paths: the mechanical one highlighted by the red arrow, and the electrical one highlighted by the green arrow. Focusing on the electrical power path, Fig. 1 also shows the presence of a reduction ratio denoted by "R_{t1}" in between the ICE and the electrical generator. This is inserted in order to achieve a proper matching between the operating regions of the two elements. Additionally, a lock-up clutch is placed in between the electric motor and the rear transmission axle of the vehicle. This lock-up clutch allows to connect or disconnect the electric motor from the transmission, thus enabling a fully-mechanical operation of the vehicle if desired. Thanks to the lock-up clutch, the inertial load associated with the electric motor can be removed when the vehicle operates in fully-mechanical mode. Downstream with respect to the lock-up clutch, two additional gears introducing another

[1]Davide Tebaldi and [2]Roberto Zanasi are with the Department of Engineering "Enzo Ferrari", University of Modena and Reggio Emilia, Italy, e-mail: davide.tebaldi@unimore.it, roberto.zanasi@unimore.it

reduction ratio denoted by "R_{t2}" are present. The purpose of this latter ratio is to make the electric motor operating regions compatible with the transmission operating regions.

In order to maximize the benefits given by the developed architecture, the *energy management problem* must be solved [2]-[8] for the considered hybrid architecture. As an example, the modeling and control of series hybrid electric agricultural tractors is addressed in [8]. In particular, two rule-based strategies are considered, having different degrees of engine and battery usage. In general, the two electric machines and the ICE must be driven so as to reduce the ICE specific fuel consumption, maintain the energy storage device state of charge within an acceptable range and satisfy the required power from the vehicle transmission system.

A control strategy for the solution of the energy management problem is proposed in this study, allowing to satisfy the requirements, which uses the concept of ICE *minimum specific consumption path*. A control strategy based on a similar concept is proposed by the authors in [9] for a hybrid architecture of the power-split eCVT type and in [15] for a series hybrid architecture. The differences of the *minimum specific consumption path* in [9] and [15] with respect to the one proposed in this paper are detailed and described in Sec. II-A.

The structure of this paper is the following: the hybrid architecture modeling is described in Sec. II with reference to the Power-Oriented Graphs (POG) technique [10], giving particular attention to the ICE *minimum specific consumption path* tool employed for the control. Sec. III describes the control strategy for the architecture, which is applied by a control logic determining the state of the vehicle (see Sec. III-A) and controlling the three power sources ICE, electric motor and electric generator (see Sec. III-B). The obtained simulation results are presented in Sec. IV. Finally, the conclusions are reported in Sec. V.

II. Modeling of the Hybrid Vehicle

Fig. 1 shows the parallel hybrid architecture analyzed in this work, whereas Fig. 2 shows the associated Simulink block scheme.

The systems in the architecture of Fig. 2 are, ordered from the top/left to the bottom/right corner, the electric machine working as a generator, the inverter that controls this machine, the energy storage device (which is the supercapacitor named C_s), the inverter that controls the electric machine working as a motor, the electric machine working as a motor, the ICE, the gearbox, the additional reduction ratio together with the lock-up clutch and, finally, the mechanical transmission system of the vehicle.

The modeling of the PMSMs employed in the architecture under consideration has been performed employing the POG technique [10]-[11]. The project has involved the usage of two industrial PMSMs. The estimation of the model parameters has been accomplished by using the machines datasheet as a starting point, by performing the system efficiency analysis [12]-[13] and by using a least square algorithm.

The two "inverter subsystems" in Fig. 2 are based on the vectorial control [14] with reference to the POG model of the PMSM.

The dynamic model of the supercapacitor has been represented by means of the POG block in the center-top part of Fig. 2.

The dynamic model of the vehicle transmission system [15] has been derived by considering the front and rear axles as a unique transmission axle, whereas the dynamic model of the lock-up clutch has been derived by applying the approach using the main and relative system dynamics described in [16].

The modeling of the ICE is performed and detailed in the next Sec. II-A.

A. Modeling of the ICE

As far as the ICE is concerned, two pieces of information are needed for the control of the considered hybrid vehicle: the maximum ICE torque $T_{ice_{max}}$ versus the ICE speed W_{ice}, together with the ICE *minimum specific consumption path*, which gives the optimal ICE torque $T_{ice_{opt}}$ expressed as a function of the ICE speed W_{ice}. Such pieces of information are graphically shown in Fig. 3, where the blue dashed curve represents the characteristic $T_{ice_{max}}$ vs W_{ice}, and the magenta dashed curve represents the ICE *minimum specific consumption path* $T_{ice_{opt}}$ vs W_{ice}. The colored areas in Fig. 3 represent portions of the ICE specific fuel consumption map for which the specific consumption is decreasing when moving from the red portions to the green portions (for which the minimum of the ICE specific consumption is achieved).

The meaning of the ICE *minimum specific consumption path* for a parallel architecture significantly differs from the one related to the power-split hybrid architecture described in [9] and to the series hybrid architecture described in [15]. The presence of a planetary gear set in power-split architectures makes both the ICE speed W_{ice} and the ICE torque T_{ice} exploitable as degrees of freedom. Similarly, the lack of a direct coupling between the ICE and the transmission in a series architectures makes both the ICE speed W_{ice} and the ICE torque T_{ice} exploitable as degrees of freedom. On the contrary, the ICE speed is always coupled to the vehicle speed in parallel architectures, meaning that it cannot be arbitrarily chosen.

It follows that the ICE *minimum specific consumption path* for a parallel architecture is *W_{ice}-dependent* and addresses the following issue: "what is the optimal ICE torque $T_{ice_{opt}}$ which minimizes the ICE specific fuel consumption over the whole ICE speed range $W_{ice} \in [W_{ice_{min}}, W_{ice_{max}}]$?".

The procedure for computing the W_{ice}-dependent *minimum specific consumption path* of a parallel hybrid architecture requires to analyze the whole ICE speed range $W_{ice} \in [W_{ice_{min}}, W_{ice_{max}}]$. For each ICE speed point W_{ice}, the ICE specific consumption map can be exploited in order to find the most suitable ICE torque T_{ice} along the y-axis, see Fig. 3, that minimizes the specific fuel consumption of the ICE at the considered ICE speed W_{ice}. This task has been carried out by a Matlab function made for this purpose,

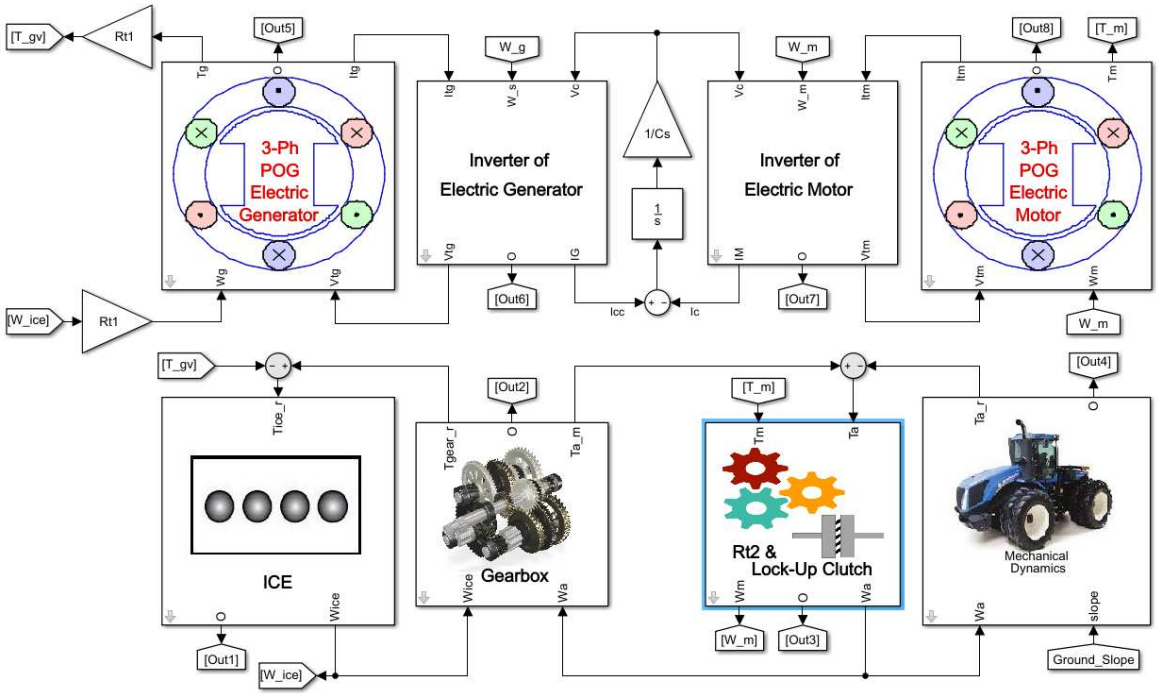

Fig. 2. Simulink block scheme of the considered parallel hybrid propulsion system.

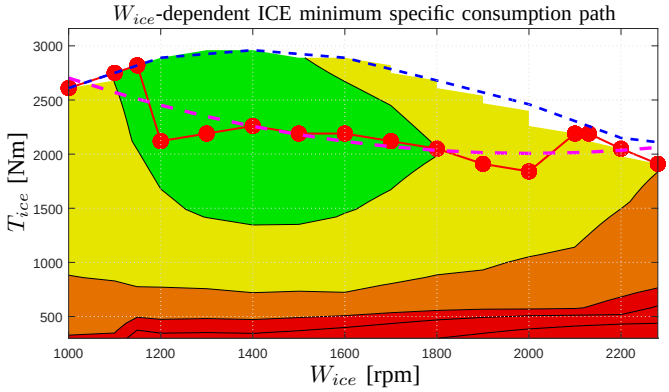

Fig. 3. ICE minimum specific consumption path dependent on the ICE speed in the operating plane (W_{ice}, T_{ice}).

and the computed minimum specific consumption points for each ICE speed W_{ice} are shown in Fig. 3 by red spots. The magenta characteristic in Fig. 3 is the actual W_{ice}-dependent *minimum specific consumption path* that will be used. The latter exhibits transitions which are less abrupt compared to those in the red path, and has been obtained using the following relation:

$$T_{ice} = p_0 + W_{ice} p_1 + W_{ice}^2 p_2, \quad \text{where} \quad \begin{cases} p_0 = 4.79 \cdot 10^3 \\ p_1 = -26.64 \\ p_2 = 0.064 \end{cases} . \quad (1)$$

As far as the ICE speed range $W_{ice} \in [0,\, W_{ice_{min}})$ is concerned, the ICE optimal torque $T_{ice_{opt}}$ giving the minimum specific consumption is assumed to be linearly increasing from $T_{ice_{opt}} = 0$ at $W_{ice} = 0$ until the beginning of the *minimum specific consumption path*, i.e. until $W_{ice} = W_{ice_{min}}$.

III. Control Strategy

In this section, the description of the control strategy developed for the parallel hybrid architecture under consideration is given. The load power demand is met using the two power paths in the system: the electrical one and the mechanical one. Therefore, the energy management problem is solved by presenting the power sources control. The available power sources are: the ICE, the electric motor and the electric generator. The control of the three power sources is handled by a control logic having two main purposes:

- A) Determination of the current *vehicle state*, see Sec. III-A;
- B) ICE, electric generator and electric motor control according to the current *vehicle state*, see Sec. III-B;

A. Determination of the vehicle state

The control logic makes a decision about the *state* of the vehicle at each time step on the basis of the current value of three *decision variables*: v_v, $T_{ice_{req}}$ and V_c, that are the vehicle speed, the torque which would be required to the ICE if there were no electrical path (fully-mechanical operating mode) and the voltage drop across the supercapacitor, respectively. From now on, variable $T_{ice_{req}}$ will be referred to as "fictitious torque required to the ICE", since it coincides with the actual ICE demanded torque iff the electrical path is disabled or the electric motor is not required to provide its contribution.

The discriminating thresholds for the three *decision variables* v_v, $T_{ice_{req}}$ and V_c are called *decision parameters*: v_{v_t}, $T_{ice_{opt}}$, $V_{c_{low}}$ and $V_{c_{up}}$. The first decision parameter v_{v_t} is a constant representing the threshold vehicle speed above

which the lock-up clutch opens, thus disabling the electrical power path and the vehicle passes in fully-mechanical operating mode. The second decision parameter $T_{ice_{opt}}$ is a time-variant parameter representing the optimal ICE torque versus the ICE speed W_{ice} given by the *minimum specific consumption path* according to (1). The third and fourth decision parameters $V_{c_{low}}$ and $V_{c_{up}}$ are two constant parameters representing the lower and upper thresholds of the voltage V_c across supercapacitor C_s, the latter being related to the supercapacitor state of charge. Because of the dynamics of the considered system, a safety range is left between $V_{c_{low}}$, $V_{c_{up}}$ and the actual minimum and maximum thresholds $V'_{c_{low}}$ and $V'_{c_{up}}$, respectively, such that:

$$V'_{c_{low}} < V_{c_{low}} \quad \text{and} \quad V'_{c_{up}} > V_{c_{up}}.$$

The considered parallel hybrid architecture is characterized by five states: States from 1 to 4 are characterized by the vehicle operating in hybrid mode, whereas State 5 is characterized by the vehicle operating in fully-mechanical mode. The entering/exiting conditions according to which the control logic makes a decision about the current vehicle state are described in Fig. 4 with the aid of a flowchart.

B. Control of the power sources

A Proportional-Integral-Derivative (PID) controller is employed to translate the ICE speed error $\Delta_{W_{ice}} = W_{ice_{des}} - W_{ice}$ into the fictitious torque $T_{ice_{req}}$ required to the ICE. Thanks to the presence of the two parallel power paths, such fictitious torque $T_{ice_{req}}$ is properly split between the *actual* torque $T_{ice_{dem}}$ demanded to the ICE and the actual torque $T_{m_{dem}}$ demanded to the electric motor depending on the vehicle state.

A proportional controller is employed to translate the supercapacitor voltage error $\Delta_{V_c} = V_{c_{ref}} - V_c$ into a desired torque for the electrical generator $T_{g_{dem}}$, in order to recharge the supercapacitor when $V_c < V_{c_{low}}$. The reference value for the supercapacitor voltage $V_{c_{ref}}$ is defined as the arithmetic mean of the upper and lower voltage thresholds $V_{c_{up}}$ and $V_{c_{low}}$, $V_{c_{ref}} = (V_{c_{up}} - V_{c_{low}})/2$.

From these considerations about the determination of the demanded torques, the reader can evince that a *torque control* is applied to the three power sources.

The *vehicle state* uniquely determines the proper torque demands $T_{ice_{dem}}$, $T_{m_{dem}}$ and $T_{g_{dem}}$ for the three power sources ICE, electric motor and electric generator in order to fulfill the requirements: minimize the ICE specific fuel consumption, satisfy the power demand coming from the transmission and make sure that the supercapacitor voltage is always confined in between the minimum and maximum acceptable thresholds $V'_{c_{low}}$ and $V'_{c_{up}}$. The five possible vehicle states characterizing the considered parallel architecture and the corresponding control actions are discussed in the following.

1) State 1: The vehicle is in this state when the fictitious torque $T_{ice_{req}}$ required to the ICE is greater than the optimal one $T_{ice_{opt}}$ and the supercapacitor is sufficiently charged to sustain the operation of the electric motor, i.e. when $V_c \geq V_{c_{low}}$, see Fig. 4. In this state, the control logic imposes the following equalities:

$$\begin{cases} \Delta_{T_{ice}} &= T_{ice_{req}} - T_{ice_{opt}} \\ T_{ice_{dem}} &= T_{ice_{opt}} \\ T_{m_{dem}} &= \left(\dfrac{\Delta_{T_{ice}}}{R_g}\right) R_{t2} \\ T_{g_{dem}} &= 0 \end{cases} \tag{2}$$

where R_g is the reduction ratio of the currently engaged gear and R_{t2} is the reduction ratio introduced by the gears placed downstream with respect to the lock-up clutch, see Fig. 1.

From (2), one can see that: the ICE actual demanded torque $T_{ice_{dem}}$ is determined so as to keep the ICE operating point along the *minimum specific consumption path*, the electric motor actual demanded torque $T_{m_{dem}}$ is determined in order to convert the additional ICE torque request $\Delta_{T_{ice}}$ into a request for the electric motor, and the electric generator actual demanded torque $T_{g_{dem}}$ is set to zero in order not to make the electric motor and the electric generator operate at the same time.

2) State 2: The vehicle is in this state when the supercapacitor must be recharged, i.e. when $V_c < V_{c_{low}}$ (see Fig. 4) in order not to cause voltage V_c to go below the minimum threshold $V'_{c_{low}}$. In this state, the control logic imposes the following equalities:

$$\begin{cases} \Delta_{V_c} &= V_{c_{ref}} - V_c \\ T_{g_{dem}} &= -K\,\Delta_{V_c} \\ \Delta_{T_{ice}} &= -T_{g_{dem}}\,R_{t1} \\ T_{ice_{dem}} &= T_{ice_{req}} + \Delta_{T_{ice}} \\ T_{m_{dem}} &= 0 \end{cases} \tag{3}$$

where K is the properly set gain of the proportional regulator converting the supercapacitor voltage error Δ_{V_c} into a torque demanded to the electric generator $T_{g_{dem}}$.

From (3), one can see that the ICE actual demanded torque $T_{ice_{dem}}$ is determined in order to fully satisfy the request $T_{ice_{req}}$ to guarantee that the ICE and thus the transmission will follow the desired speed profile and in order to provide the electric generator with the demanded torque level $T_{g_{dem}}$. The electric motor actual demanded torque $T_{m_{dem}}$ is set to zero in order not to make the electric motor and the electric generator operate at the same time, whereas the electric generator actual demanded torque $T_{g_{dem}}$ is determined in order to properly recharge the supercapacitor.

3) State 3: The vehicle is in this state when the fictitious ICE demanded torque $T_{ice_{req}}$ is lower than the optimal one $T_{ice_{opt}}$ and the supercapacitor voltage V_c is lower than the upper threshold $V_{c_{up}}$, see Fig. 4. In this state, the control logic imposes the following equalities:

$$\begin{cases} \Delta_{T_{ice}} &= T_{ice_{opt}} - T_{ice_{req}} \\ T_{g_{dem}} &= -\dfrac{\Delta_{T_{ice}}}{R_{t1}} \\ T_{ice_{dem}} &= T_{ice_{opt}} \\ T_{m_{dem}} &= 0 \end{cases} \tag{4}$$

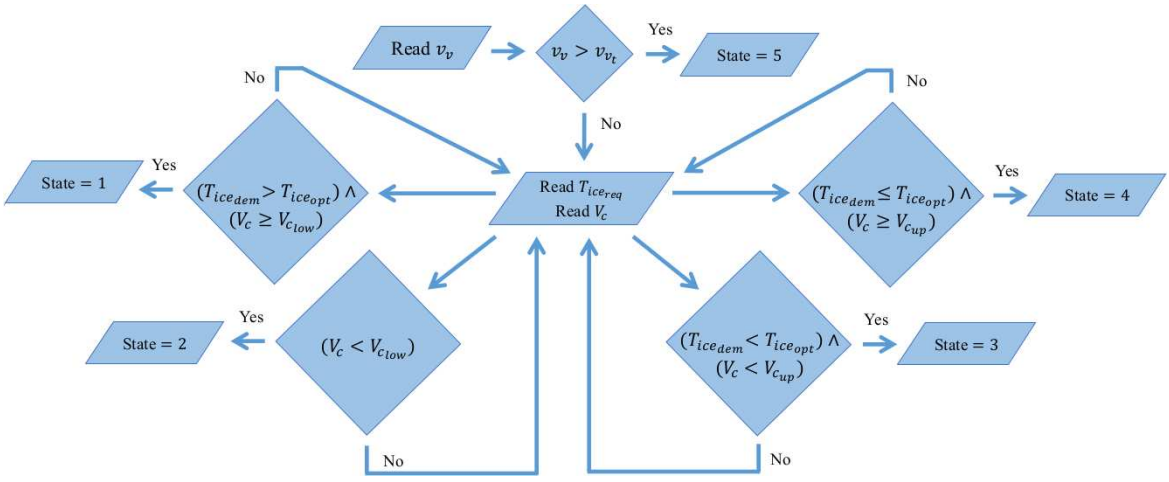

Fig. 4. Flowchart describing the determination of the current vehicle state.

From (4) one can see that the ICE actual demanded torque $T_{ice_{dem}}$ is determined so as to keep the ICE operating point along the *minimum specific consumption path* and the electric motor actual demanded torque $T_{m_{dem}}$ is set to zero, in order not to make the electric motor and the electric generator operate at the same time.

The electric generator actual demanded torque $T_{g_{dem}}$ is determined in order exploit the additional ICE torque $\Delta_{T_{ice}}$, which is not required by the transmission, in order to recharge the supercapacitor. The philosophy behind this choice is the following one: since the transmission torque request is such as to make the ICE torque lower than the optimal one, thus rising the specific fuel consumption of the ICE, and since the supercapacitor voltage is lower than $V_{c_{up}}$, it makes sense to improve the specific fuel consumption of the ICE by setting the ICE torque equal to the optimal one and to exploit the ICE extra torque to recharge the supercapacitor as much as its characteristics allow.

4) State 4: The vehicle is in this state when the fictitious ICE demanded torque $T_{ice_{req}}$ is lower than or equal to the optimal one $T_{ice_{opt}}$ and the supercapacitor voltage V_c is greater than or equal to the upper threshold $V_{c_{up}}$, see Fig. 4. In this state, the control logic imposes the following equalities:

$$\begin{cases} T_{ice_{dem}} &= T_{ice_{req}} \\ T_{m_{dem}} &= 0 \\ T_{g_{dem}} &= 0 \end{cases} \tag{5}$$

From (5), one can notice that the ICE actual demanded torque $T_{ice_{dem}}$ coincides with the fictitious torque $T_{ice_{req}}$ which would be required to the ICE if the electrical path were disabled, since both the electric motor and the electric generator actual demanded torques $T_{m_{dem}}$ and $T_{g_{dem}}$ are set to zero. $T_{m_{dem}}$ is set to zero because there is no need to perform torque compensation as the ICE demanded torque is lower than the optimal one; $T_{g_{dem}}$ is set to zero because it is not possible to exploit the fact that the ICE demanded torque is lower than the optimal one in order to recharge the supercapacitor, since it cannot be recharged any further (because $V_c \geq V_{c_{up}}$ is already verified, and $V_c < V'_{c_{up}}$ has to be guaranteed).

5) State 5: The vehicle is in this state when the vehicle speed v_v is greater than threshold v_{v_t} ($v_v > v_{v_t}$), therefore the control logic opens the lock-up clutch to disable the electrical power path. In this case, the control logic imposes the following equalities:

$$\begin{cases} T_{ice_{dem}} &= T_{ice_{req}} \\ T_{m_{dem}} &= 0 \\ T_{g_{dem}} &= 0 \end{cases} \quad \text{if} \quad V_c \geq V_{c_{ref}}$$

$$\begin{cases} \Delta_{T_{ice}} &= T_{ice_{max}} - T_{ice_{req}} \\ T_{ice_{dem}} &= T_{ice_{max}} \\ T_{g_{dem}} &= -\dfrac{\Delta_{T_{ice}}}{R_{t1}} \\ T_{m_{dem}} &= 0 \end{cases} \quad \text{if} \quad V_c < V_{c_{ref}} \tag{6}$$

Relations (6) highlight that State 5 is decoupled into two substates:

- When $V_c \geq V_{c_{ref}}$, the ICE actual demanded torque $T_{ice_{dem}}$ is simply set to be equal to the ICE fictitious demanded torque $T_{ice_{req}}$, since this is exactly the case of fully-mechanical operating mode. Indeed, it is fully up to the ICE to satisfy the transmission torque request. The electric motor and generator actual demanded torques $T_{m_{dem}}$ and $T_{g_{dem}}$ are therefore set to zero.
- When $V_c < V_{c_{ref}}$, the ICE actual demanded torque $T_{ice_{dem}}$ is set to the maximum torque $T_{ice_{max}}$ available at the current ICE speed W_{ice} until $V_c = V_{c_{ref}}$. The electric motor actual demanded torque $T_{m_{dem}}$ is still set to zero, as the lock-up clutch is open. The electric generator actual demanded torque $T_{g_{dem}}$ is determined in order to exploit the additional ICE torque $\Delta_{T_{ice}}$ so as to recharge the supercapacitor, in order for it to be fully operative when the vehicle leaves State 5 and enters in hybrid mode again.

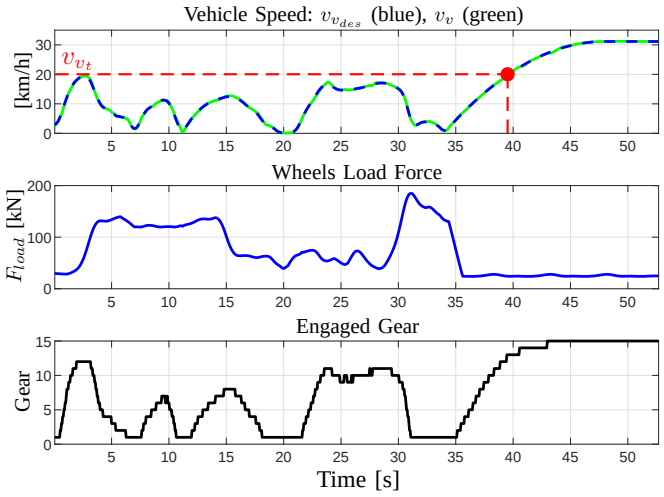

Fig. 5. Desired and Actual Vehicle Speed; Wheels Load Force; Engaged Gear.

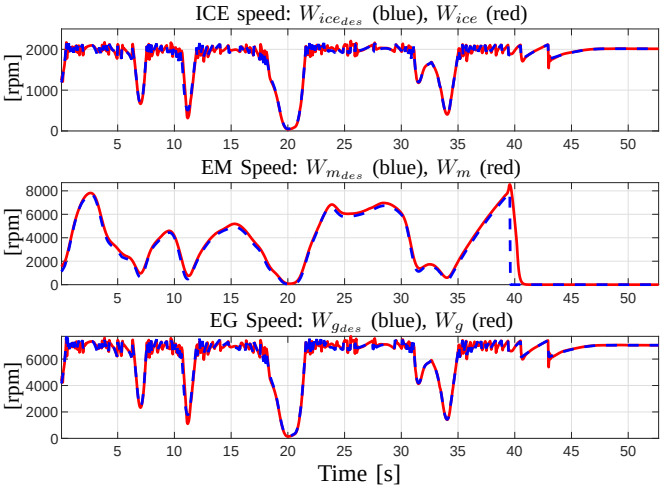

Fig. 6. Desired and actual ICE speed; Desired and Actual Electric Motor Speed; Desired and Actual Electric Generator Speed; .

IV. Simulations

The architecture whose Simulink scheme is shown in Fig. 2 has been simulated by making the tractor follow a determined speed profile. During the simulation, the vehicle is subject to a wheels load force associated with the tractor operation. The parameters values inserted in the model could not be shown because of trade secret. The simulation results are provided in Fig. 5, Fig. 6, Fig. 7, Fig. 8 and Fig. 9.

The upper subplot in Fig. 5 reports the desired vehicle speed profile $v_{v_{des}}$ (blue dashed line) and the actual vehicle speed v_v (green line). The middle subplot shows the wheels load force F_{load} that the vehicle is subject to during its operation. The lower subplot in Fig. 5 reports the gear signal, denoting which gear is engaged at different vehicle speed. The red dashed line in the upper subplot highlights the vehicle speed threshold $v_{v_t} = 20$ [km/h] above which the vehicle enters State 5, denoting the operation in fully-mechanical mode. This operating mode is activated when the tractor is traveling by road. In this case, the tractor is not operating on the field and is subject to a lighter load force, therefore no torque compensation by the electric motor is needed.

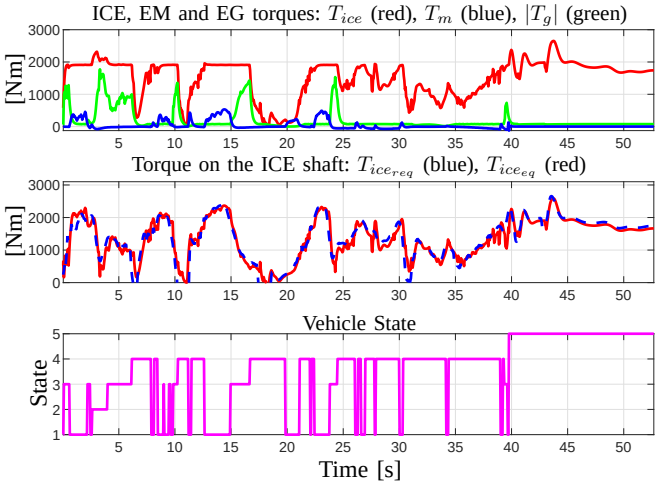

Fig. 7. ICE, EM and EG torques reported on the ICE shaft; Fictitious and equivalent torque on the ICE shaft; State of the vehicle.

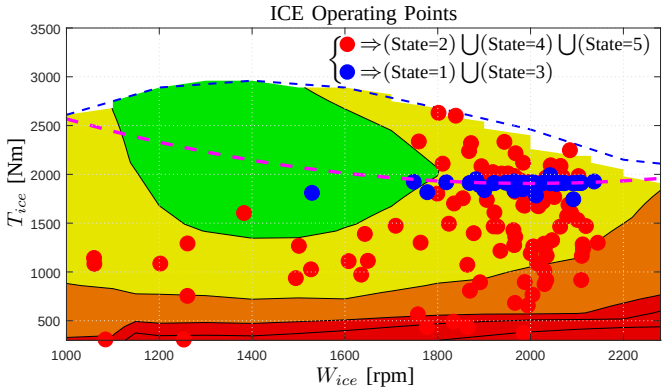

Fig. 8. Operating points of the ICE on the specific fuel consumption map.

The three subplots in Fig. 6 show, from top to bottom, the desired and actual ICE speeds $W_{ice_{des}}$ and W_{ice}, the desired and actual electric motor speeds $W_{m_{des}}$ and W_m, the desired and actual electric generator speeds $W_{g_{des}}$ and W_g, where the desired profiles are plotted in blue dashed lines and the actual profiles are plotted in red lines. The actual speed profiles in Fig. 5 and Fig. 6 agree with the desired ones, showing how the joint contribution of the three power sources ICE, electric motor and electric generator, which are properly controlled thanks to the developed control strategy, effectively satisfies the transmission power demand.

The upper subplot in Fig. 7 reports: the actual ICE torque T_{ice} (red curve), the equivalent electric motor torque T_m reported on the ICE shaft through the currently engaged gear R_g and ratio R_{t2} (blue curve) and the modulus of the equivalent electric generator torque T_g reported on the ICE shaft through ratio R_{t1} (green curve). The actual values of T_g are negative, denoting the operation of this electric machine as a generator. The middle subplot in Fig. 7 reports the fictitious ICE required torque $T_{ice_{req}}$ that the ICE should provide in fully-mechanical operating mode and the equivalent motive torque $T_{ice_{eq}}$ available on the ICE shaft, which is given by the algebraic sum of the three power sources torques reported in the upper subplot of Fig. 7. The lower subplot in Fig. 7

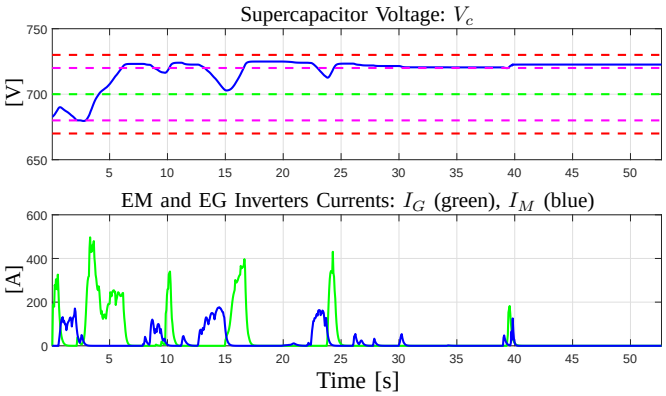

Fig. 9. Supercapacitor voltage; Electric Motor and Electric Generator Inverters Currents.

shows how the vehicle state changes during the simulation. The current vehicle state, determined by the control logic according to the algorithm described in Fig. 4, uniquely determines the ICE torque T_{ice}, the electric motor torque T_m and the electric generator torque T_g, according to the strategy presented in Sec. III-B.

Fig. 8 reports the operating points (W_{ice}, T_{ice}) of the ICE on its specific consumption map. It can be noticed that, when the vehicle is operating in States 1 and 3, the ICE torque T_{ice} coincides with the optimal ICE torque $T_{ice_{opt}}$ according to (2) and (4). In these states, the ICE operating points are confined around the *minimim specific consumption path* in (1), see the blue spots in Fig. 8. The red spots in Fig. 8 show that, when the vehicle is operating in the remaining States 2, 4 and 5, the ICE leaves the *minimum specific consumption path* as required by the control logic, see (3), (5) and (6). Metrics giving the comparison of the obtained specific fuel consumption of the ICE with the one given by the non-hybrid agricultural tractor could not be shown because of trade secret.

Finally, the blue curve in the upper subplot of Fig. 9 represents the supercapacitor voltage V_c. The maximum, upper, reference, lower and minimum thresholds $V'_{c_{up}}$, $V_{c_{up}}$, $V_{c_{ref}}$, $V_{c_{low}}$ and $V'_{c_{low}}$ are shown in upper dashed red, upper dashed magenta, dashed green, lower dashed magenta and lower dashed red lines, respectively. The lower subplot in Fig. 9 reports the electric motor inverter current I_M discharging the supercapacitor (blue curve), as well as the electric generator inverter current I_G recharging the supercapacitor (green curve). By looking at Fig. 7 and Fig. 9, one can notice that the electric motor inverter current I_M is different from zero only in correspondence of those time frames where the electric motor torque T_m is different from zero, as expected. A similar consideration can be made as far as the electric generator inverter current I_G and torque T_g are concerned as well.

V. Conclusions

This paper has concerned the modeling, the control and the simulation of a parallel hybrid architecture. The modeling of the physical elements has been described with reference to the Power-Oriented Graphs technique. An effective control strategy for solving the energy management problem has been shown, which allows to minimize the specific fuel consumption of the ICE, control the supercapacitor state of charge and satisfy the transmission power demand. The efficacy of the control strategy has been shown thanks to some simulation results of the considered parallel hybrid agricultural tractor.

References

[1] W. Hong-xing, K. Bao-quan, L. Li-yi, "The Research for Power Matching Strategy of Parallel Hybrid Vehicle", IEEE Vehicle Power and Propulsion Conference (VPPC), Harbin, China, Sep. 3-5, 2008.

[2] A. Hossein Eghbali, B. Asaei, "Efficient Control Strategy for Reducing Fuel Consumption in Parallel Hybrid Electric Vehicles, Based on Engine and Electric Motor Efficient Operating Points", IEEE Vehicle Power and Propulsion Conference (VPPC), Dearborn, MI, USA, Sep. 7-10, 2009.

[3] A. Kahrobaeian, R. Amiri, "Comparative Investigation of Charge-Sustaining and Fuzzy Logic Control Strategies in Parallel Hybrid Electric Vehicles", IEEE Vehicle Power and Propulsion Conference (VPPC), Dearborn, MI, USA, Sep. 7-10, 2009.

[4] L. Qingkai, Z. Zhiguo, D. Haifeng, "Energy Management Strategy for Single Driveshaft Parallel Hybrid Electric Vehicle Based on Torque Control", IEEE Vehicle Power and Propulsion Conference (VPPC), Dearborn, MI, USA, Sep. 7-10, 2009.

[5] S. A. Zulkifli, N. Saad, "Split-Parallel In-Wheel-Motor Retrofit Hybrid Electric Vehicle", IEEE International Power Engineering and Optimization Conference (PEOCO), Melaka, Malaysia, Jun. 6-7, 2012.

[6] D. Sigmund, A. Lohner, M. Böh, "Simulation-based development of an energy-management-system for a drive train of a parallel hybrid electric vehicle", 16th International Power Electronics and Motion Control Conference and Exposition, Antalya, Turkey, Sep. 21-24, 2014.

[7] Yu-H. Cheng, Ching-M. Lai, J. Teh, "Memetic Algorithm for Fuel Economy and Low Emissions Parallel Hybrid Electric Vehicles", IEEE 8th International Conference on Awareness Science and Technology (ICAST), Taichung, Taiwan, Nov. 8-10, 2017.

[8] C. Jia, W. Qiao, L. Qu, "Modeling and Control of Hybrid Electric Vehicles: A Case Study for Agricultural Tractors", IEEE Vehicle Power and Propulsion Conference (VPPC), Chicago, IL, USA, Aug. 27-30, 2018.

[9] D. Tebaldi, R. Zanasi, "Modeling and Control of a Power-Split Hybrid Propulsion System", IEEE 45th Annual Conference of the Industrial Electronics Society, Lisbon, Portugal, Oct. 14-17, 2019.

[10] R. Zanasi, "The Power-Oriented Graphs Technique: System modeling and basic properties", IEEE Vehicle Power and Propulsion Conference, Lille, France, Sep. 1-3, 2010.

[11] M. Fei, R. Zanasi, F. Grossi, "Modeling of Multi-phase Permanent Magnet Synchronous Motors under Open-phase Fault Condition", IEEE International Conference on Control and Automation (ICCA), Santiago, Chile, Dec. 19-21, 2011.

[12] R. Zanasi, D. Tebaldi, "Power Flow Efficiency of Linear and Nonlinear Physical Systems", IEEE European Control Conference (ECC), Naples, Italy, Jun. 25-28, 2019.

[13] R. Zanasi, D. Tebaldi, "Study of the Bidirectional Efficiency of Linear and Nonlinear Physical Systems", IEEE 45th Annual Conference of the Industrial Electronics Society, Lisbon, Portugal, Oct. 14-17, 2019.

[14] R. Zanasi, F. Grossi, "Vectorial Control of Multi-phase Synchronous Motors using POG Approach", 35th Annual Conference of IEEE Industrial Electronics, Porto, Portugal, Nov. 3-5, 2009.

[15] D. Tebaldi, R. Zanasi, "Modeling Control and Simulation of a Series Hybrid Propulsion System", IEEE Vehicle Power and Propulsion Conference (VPPC), Gijón, Spain, Oct. 26-29, 2020.

[16] R. Zanasi, G. Sandoni, R. Morselli, Simulation of variable Dynamic Dimension Systems: The Clutch Example", European Control Conference (ECC), Porto, Portugal, Sep. 4-7, 2001.